



Development of Amperometric Biosensor for the Detection of *Vibrio vulnificus* as Biological Weapon

Harish Kumar*, Bhawana Gupta

Department of Chemistry, Material Science & Electrochemistry Laboratory, Chaudhary Devi Lal University, Sirsa - 125 055, Haryana, India.

Received 09th December 2015; Revised 12th January 2016; Accepted 11th March 2016

ABSTRACT

The rapid, unambiguous detection and identification of biological warfare agents (BWAs) with early warning signals for detecting a possible biological attack is a major challenge for military, health and other government defense agencies. The current research is focused on the development of amperometric biosensors for the detection of BWA. For this purpose, a carbon-based (graphene) working electrode containing enzyme alkaline phosphatase, cellulose acetate and poly (vinyl pyrrolidone), ferrocene, horseradish peroxidase, aqueous potassium hydroxide was fabricated. It is then combined with Ag/AgCl reference and platinum (auxiliary) electrode to form a three-electrode based electrochemical biosensor for the electrochemical detection of *Vibrio vulnificus* as BWA in the presence and absence of Fe_3O_4 nanoparticles. Fe_3O_4 nanoparticles were synthesized by sol-gel technique and were characterized by ultraviolet-visible, Fourier transform infrared, transmission electron microscopy, and X-ray diffraction techniques. Change in current response and open circuit potential (OCP) values help in the detection of BWA in presence and absence of Fe_3O_4 nanoparticles. Effects of temperature, stirring and Fe_3O_4 nanoparticles on the BWA have also been investigated. Heating of BWA to 70.0°C for 6.0 h and the addition of Fe_3O_4 nanoparticles (50 μ l/ml) at room temperature has the same effect, i.e., both results in the killing of BWA resulting in the decrease of OCP value.

Key words: Biological warfare agents, Amperometric biosensors, Sol-gel method, Fe_3O_4 nanoparticles, *Vibrio vulnificus*.

1. INTRODUCTION

Bioterrorism is the use of a biological weapon (bacteria, virus or spores) on human life as a weapon of mass infection. It ultimately proves more powerful than a chemical or a nuclear weapon because it works silently and its effects can be far-reaching and uncontrollable. List of pathogenic bacteria that can be considered as possible biological warfare agents (BWA) is unending [1]. Highly dangerous include botulinum toxin, *Francisella tularensis*, *Salmonella typhimurium*, *Staphylococcus epidermis*, *Vibrio vulnificus*, and *Yersinia pestis*. Other bio-agents, like *Venezuelan equine encephalitis*, Marburg, *Ebola*, and influenza viruses are of lesser importance, despite the fact, that infections with these viruses are serious and mortality is relatively high, but due to the difficulty in their preparation, their position on the list of BWA is lower. First, evidence of bioterrorism came into existence, in 1979, when doctors presented a report of mass civilian death due to *Bacillus anthracis* pneumonia, i.e., due to inhalation of anthrax. A person

exposed to *B. anthracis* died immediately. The bacilli of anthracis multiply rapidly in the body and produce a harmful toxin that stops the process of breathing.

On the other hand, *V. vulnificus* can also be used as BWA in coastal areas. *V. vulnificus* can cause disease in those who eat contaminated seafood or have an open wound that is exposed to seawater. *V. vulnificus* typically causes a severe and life-threatening illness characterized by fever and chills, decreased blood pressure (septic shock), and blood-tinged blistering skin lesions (hemorrhagic bullae). In comparison with chemical warfare agents, BWA production is much cheaper and terrorist or military attack with BWA is more effective in the range of hazard area and in the number of expected casualties. The infectious dose (ID) (amount of organism needed for infection outbreak) is different for every agent. Usually, the intake of aerosol (particles 1-10 μ m) through lung is able to evocate disease with a lower ID for the given BWA.

*Corresponding Author:
E-mail: harimoudgill@gmail.com

Different types of electrochemical biosensors which are in common practice are potentiometric, conductometric, amperometric, and impedimetric [2-5]. Out of these, amperometric biosensors are more common in practice and are usually based on ion-selective electrodes. These are three-electrode based electrochemical systems which are attached with electrochemical detectors which measure the changes in ion concentration during reaction taking place in the bio-recognition layer. The advantage of amperometric biosensors over other biosensors is that they are highly sensitive, rapid, linear concentration dependence and inexpensive [6]. Amperometric biosensors aimed at microbial analysis have been reported by different researchers [7-11].

First biosensors used pH glass electrode with enzymes captured in a suitable membrane. In potentiometric immune-sensor electrochemical biosensor, enzyme-labeled antibodies are used. The most common labeling enzymes are urease, glucose oxidase or alkaline phosphatase, which are able to change either pH or ionic strength in the course of the detection [12]. Very popular semiconductor-based biosensors are light-addressable potentiometric sensors (LAPS). Due to their small size and possible multichannel arrangement, these devices seem to be very convenient for simultaneous analysis of several analytes [13]. The LAPS immune-sensors were used to detect *F. tularensis* [14] with a limit of detection (LOD) at 3.4×10^3 cells ml^{-1} and *Bacillus melitensis* with LOD equal to 6×10^3 cells ml^{-1} during the 1 h incubation time [15]. A better LOD was achieved for *Escherichia coli* DH5 a strain [16], the secondary antibody specific against *E. coli* labeled with urease was used and LOD of 10 cells ml^{-1} for 1.5 h assay time was claimed.

In continuation to our earlier study [17], in this paper, we have focused on the fabrication of electrochemical biosensor for the detection of *V. vulnificus* as BWA.

2. MATERIALS AND METHODS

Samples of disease-causing bacteria, i.e., *V. vulnificus* (Microbial Type Culture Collection [MTCC] No. 1145) were collected from MTCC, Institute of Microbial Technology, Chandigarh.

Different steps used for the electrochemical detection of disease causing bacteria are:

- i. Preparation of bacterial strain: The bacterial test organism *V. vulnificus* was grown in nutrient broth for 24 h at 37°C. A sodium phosphate buffer solution of pH 7.0 was prepared to hold these disease causing bacteria at a very low temperature, i.e., 4°C
- ii. Synthesis of Fe_3O_4 nanoparticles and graphene: Fe_3O_4 nanoparticles were synthesized by Sol-gel technique. In this technique, a metal salt solution having ferric chloride is added dropwise

in a mixture of tetraethyl orthosilicate in ethanol. Reduced graphene was synthesized by well-known Hummers method

- iii. Characterization of Fe_3O_4 nanoparticles and graphene: Characterization of Fe_3O_4 nanoparticles and graphene were carried out by using ultraviolet (UV)-visible spectroscopy, Fourier transform infrared (FTIR) technique, X-ray diffraction (XRD) study and transmission electron microscopy (TEM) techniques
- iv. Fabrication of working test electrode: A carbon paste (graphene) working electrode was fabricated for the electrochemical determination of biological warfare. The slurry was prepared by mixing reduced graphene, alkaline phosphatase, cellulose acetate, ferrocene, horseradish peroxidase (HRP), aqueous potassium hydroxide (KOH) and poly (vinyl pyrrolidone) (PVP). This slurry was filled in working test electrode with the help of luggin capillary. A copper wire is dipped from outside in the slurry for making electrical connections
- v. Fabrication of three electrodes based electrochemical cell: Three electrodes based electrochemical cell was fabricated having three electrodes, i.e. a working test electrode (cellulose acetate, PVP bound carbon paste electrode), Ag/AgCl reference electrode and a platinum electrode acting as an auxiliary electrode for the electrochemical determination of disease causing pathogen (Figure 1)
- vi. Electrochemical characterization: Three electrodes based electrochemical cell is connected to the instrument electrochemical workstation PGSTAT 128N, Metrohm Autolab attached to a PC and digital controlled water bath to maintain constant temperature. Electrochemical measurement experiments were performed on a pathogenic bacteria *V. vulnificus* and change in open circuit potential (OCP), current (nA) and potential values were recorded at different conditions.

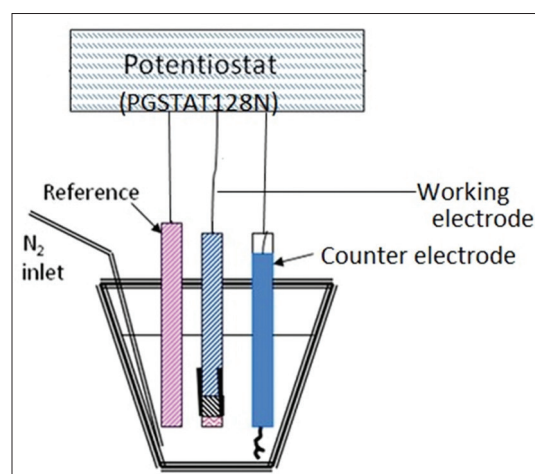


Figure 1: Electrochemical biosensor for the detection of biological warfare agent.

For the electrochemical characterization, 3×10^7 CFU of *V. vulnificus* in 50.0 ml of phosphate buffered saline (PBS) buffer solution was used. Four different samples were prepared, i.e., pure PBS buffer solution as sample 1, PBS buffer solution with 3×10^7 CFU of *V. vulnificus* as sample 2, PBS buffer solution with Fe₃O₄ nanoparticles as sample 3 and PBS buffer solution with Fe₃O₄ nanoparticles and 3×10^7 CFU of *V. vulnificus* as sample 4.

The above samples were kept under the following two observations:

- Heating at a constant temperature of 70°C without stirring for 6 h
- Continuous stirring for 6 h at room temperature.

After 6.0 h, we have recorded the current and potential values with the help of three electrodes based electrochemical cell connected to the instrument PGSTAT 128N, Metrohm Autolab, Netherland.

3. RESULTS

The result of electrochemical characterization on *V. vulnificus* is recorded in the form of Tables 1 and 2 and

Table 1: OCP values of stirred samples of *V. vulnificus*.

Samples	OCP values (V) at 0.0 h	OCP values (V) after 6.0 h
Pure PBS solution	0.524	0.542
PBS solution with 3.0×10^7 CFU of <i>V. vulnificus</i>	0.238	0.261
PBS solution with Fe ₃ O ₄ nanoparticles	0.747	0.753
PBS solution with Fe ₃ O ₄ nanoparticles and 3.0×10^7 CFU of <i>V. vulnificus</i>	0.226	0.253

V. vulnificus=*Vibrio vulnificus*, OCP=Open circuit potential

Table 2: The OCP values of heated samples of *V. vulnificus*.

Samples	OCP values (V) at 0.0 h	OCP values (V) after 6.0 h
Pure PBS solution	0.524	0.542
PBS solution with 3.0×10^7 CFU of <i>V. Vulnificus</i>	0.240	0.185
PBS solution with Fe ₃ O ₄ nanoparticles	0.747	0.753
PBS solution with Fe ₃ O ₄ nanoparticles and 3.0×10^7 CFU of <i>V. vulnificus</i>	0.228	0.180

V. vulnificus=*Vibrio vulnificus*, OCP=Open circuit potential, PBS=Phosphate buffered saline

Figures 2-8. Table 1 shows OCP values of unstirred and after 6.0 h of continuous stirring. Table 2 shows

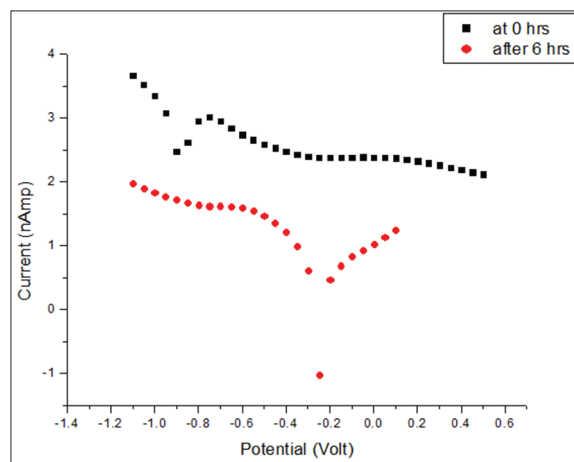


Figure 2: Current versus potential behavior of pure phosphate buffered saline buffer solution at 0.0 and after 6.0 h of stirring.

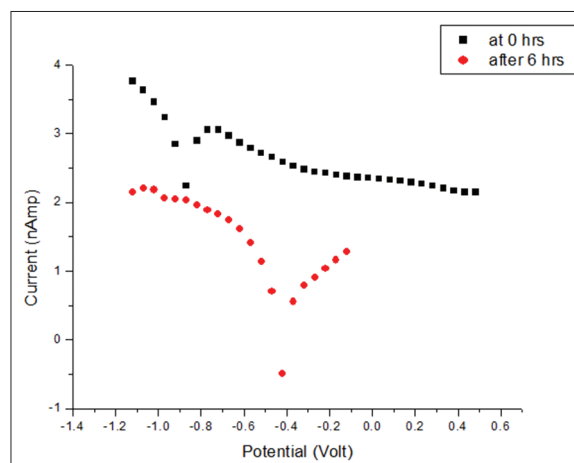


Figure 3: Current versus potential behavior of phosphate buffered saline buffer solution in the presence of Fe₃O₄ nanoparticles ($50.0 \mu\text{l ml}^{-1}$) at 0.0 and after 6.0 h of stirring.

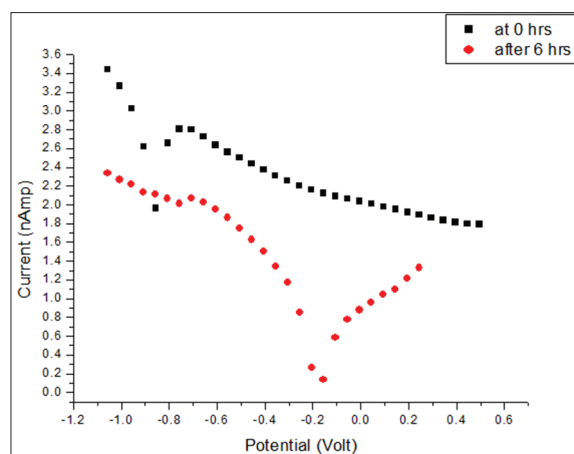


Figure 4: Current versus potential behavior of phosphate buffered saline buffer solution with *Vibrio vulnificus* at and after 6.0 h of stirring.

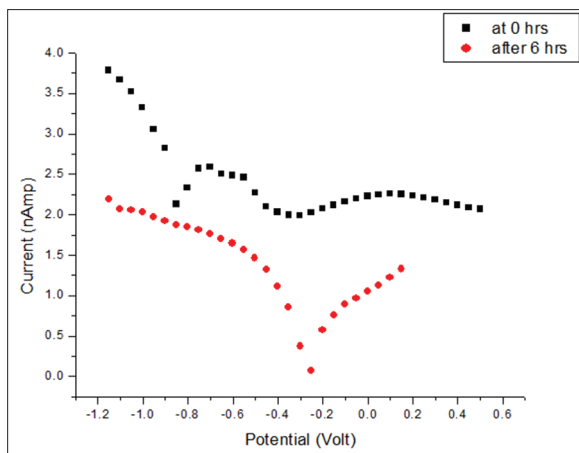


Figure 5: Current versus potential behavior of phosphate buffered saline buffer solution in the presence of *Vibrio vulnificus* and Fe_3O_4 nanoparticles ($50.0 \mu\text{l ml}^{-1}$) at 0.0 and after 6.0 h of stirring.

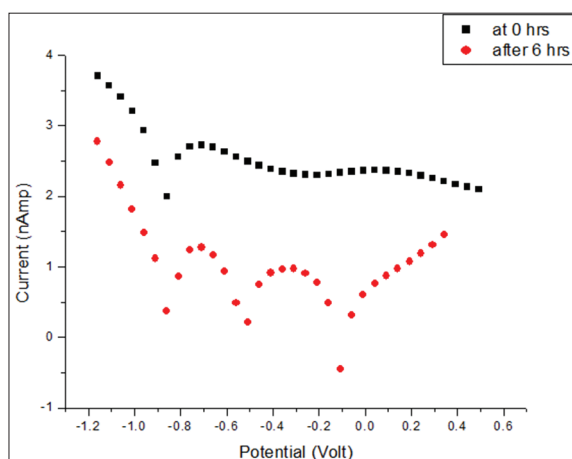


Figure 7: Current versus potential behavior of phosphate buffered saline buffer solution in the presence of Fe_3O_4 nanoparticles ($50.0 \mu\text{l ml}^{-1}$) at 0.0 and after 6.0 h of heating.

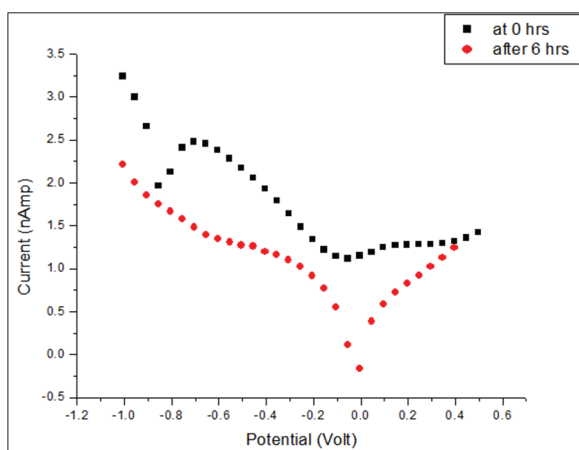


Figure 6: Current and potential behavior of pure phosphate buffered saline buffer solution at 0.0 and after 6.0 h of heating.

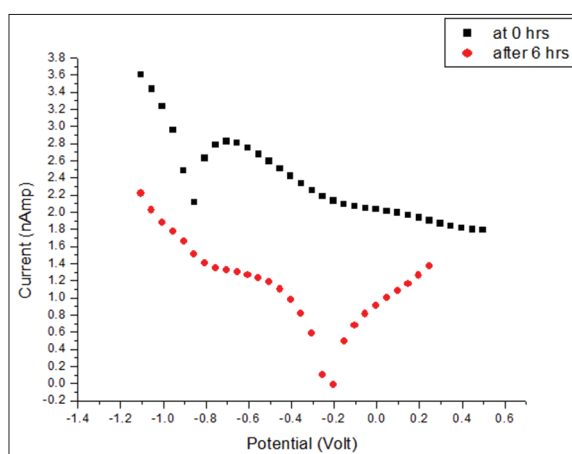


Figure 8: Current versus potential behavior of phosphate buffered saline buffer solution with *Vibrio vulnificus* at and after 6.0 h of heating.

the OCP values of four heated samples at 0.0 and at 6.0 h.

Figure 1 shows electrochemical biosensor for the detection of BWA. Figure 2 shows current and potential values of pure PBS buffer solution at 0.0 and after 6.0 h of stirring at room temperature. Figure 3 shows current and potential behavior of PBS buffer solution in the presence of *V. vulnificus* at 0.0 and after 6.0 h of stirring at room temperature. Figure 4 shows current and potential behavior of PBS buffer solution in the presence of Fe_3O_4 nanoparticles ($50.0 \mu\text{l ml}^{-1}$) at 0.0 and after 6.0 h of stirring at room temperature. Figure 5 shows current and potential behavior of PBS buffer solution in the presence of *V. vulnificus* and Fe_3O_4 nanoparticles ($50.0 \mu\text{l ml}^{-1}$) at 0.0 and after 6.0 h of stirring at room temperature.

Figure 6 shows current and potential values of pure PBS buffer solution at 0.0 and after 6.0 h of heating at

70°C . Figure 7 shows current and potential behavior of PBS buffer solution in the presence of *V. vulnificus* at 0.0 and after 6.0 h of heating at 70.0°C . Figure 8 shows current and potential behavior of PBS buffer solution in the presence of Fe_3O_4 nanoparticles ($50.0 \mu\text{l ml}^{-1}$) at 0.0 and after 6.0 h of heating at 70.0°C . Figure 9 shows current and potential behavior of PBS buffer solution in the presence of *V. vulnificus* and Fe_3O_4 nanoparticles ($50.0 \mu\text{l ml}^{-1}$) at 0.0 and after 6.0 h of heating at 70.0°C .

Figure 10 shows UV-visible spectra of Fe_3O_4 metal nanoparticles synthesized by sol-gel technique as a function of wavelength. Figure 11 shows FTIR spectra (Thermo-USA, FTIR-3800) in the wavelength range of $400\text{-}4000 \text{ cm}^{-1}$ of Fe_3O_4 metal nanoparticles synthesized by sol-gel technique. Figure 12 shows XRD pattern of Fe_3O_4 metal nanoparticles synthesized by sol-gel technique. Figure 13 shows TEM images

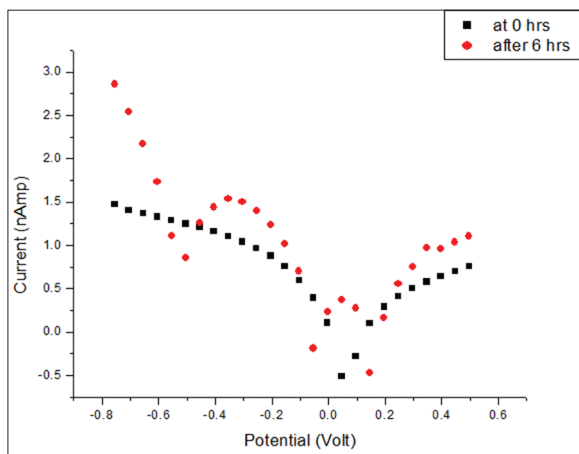


Figure 9: Current versus potential behavior of phosphate buffered saline buffer solution in the presence of *Vibrio vulnificus* and Fe_3O_4 nanoparticles ($50.0 \mu\text{l ml}^{-1}$) at 0.0 and after 6.0 h of heating.

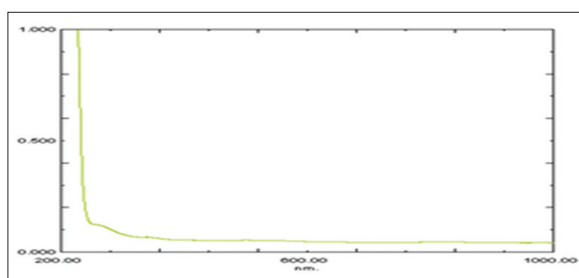


Figure 10: Ultraviolet-visible spectra of Fe_3O_4 nanoparticles.

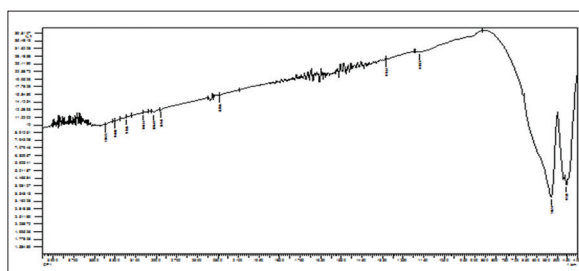


Figure 11: Fourier transform infrared spectra of Fe_3O_4 nanoparticles.

of Fe_3O_4 metal nanoparticles synthesized by sol-gel technique.

4. DISCUSSION

The UV absorption band of Fe nanoparticles (Figure 10) was observed in the wavelength range of 330-450.0 nm which may be due to the absorption and scattering of light by iron nanoparticles [18,19]. The low absorption band at a wavelength of 410.0 nm may be due to the formation of least agglomerated Fe_3O_4 nanoparticles. Further, no additional peaks were observed corresponding to alcohol which indicates that the iron nanoparticles were not encapsulated by ethanol, and they only acted as a soft template.

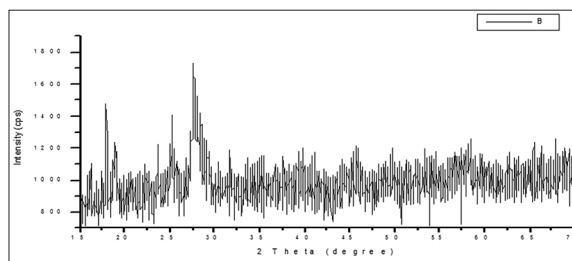


Figure 12: X-ray diffraction pattern of Fe_3O_4 nanoparticles.

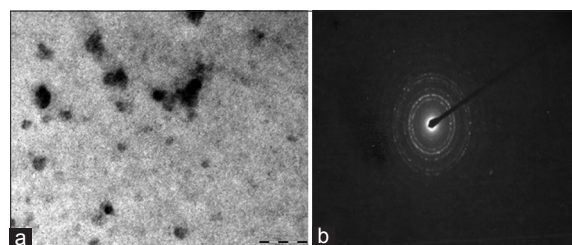


Figure 13: (a) Transmission electron microscopy images of Fe_3O_4 nanoparticles, (b) diffraction pattern of Fe_3O_4 nanoparticles

An absorption peak at 3440 cm^{-1} in the FTIR spectrum of iron oxide nanoparticles (Figure 11), (characteristic peak of OH stretching vibration) confirms the presence of some amount of ferric hydroxide in Fe_3O_4 [20,21]. The other two distinct peaks at 565 and 421.0 cm^{-1} are due to the vibrations of $\text{Fe}^{2+}-\text{O}^{2-}$ and $\text{Fe}^{3+}-\text{O}^{2-}$ respectively [22]. Another peak (sharp and high intensity) at 565 cm^{-1} indicates the presence of high degree of crystallinity in the Fe_3O_4 nanoparticles. The characteristic absorption bands at 565 and 421 cm^{-1} confirm the presence of spinel structure in Fe_3O_4 nanoparticles. FTIR spectroscopic technique was carried out to ascertain the purity and nature of ferrite metal nanoparticles synthesized by sol-gel technique.

The reflection peak at $2\theta=35.60^\circ$ confirm spinel phase of ferrite (Fe_3O_4) nanoparticles (JCPDS, PDF cards 3-864 and 22-1086) (Figure 12). The diffractions peaks of the ferrite nanoparticles were observed at $2\theta=30.18^\circ$ ($d=0.297 \text{ nm}$), 35.61° ($d=0.253 \text{ nm}$), 43.27° ($d=0.209 \text{ nm}$), 53.56° ($d=0.171 \text{ nm}$), and 57.11° ($d=0.162 \text{ nm}$) [23]. The peaks at an angle of 30.18° (220), 35.612° (311), 43.278° (400), 53.569° (422), 57.118° (511), and 62.655° (440) correspond to Fe_3O_4 . The average particle size of ferrite nanoparticles has been calculated using well-known Scherrer equation [24] and was found to be 31.0 nm . Further, diffraction peak broadening confirms the formation of the ultrafine ferrite nanoparticles.

Structural and optical properties of Fe_3O_4 metal nanoparticles were determined by using TEM of made Morgagni 268 D, FEI Philips at a resolution of 2 \AA from Electron Microscope Facility (SAIF), AIIMS, New Delhi (Figure 13a). The TEM images reveal self-

organized network like morphology of ferrite (Fe_3O_4) nanoparticles which are almost identical in shape and appear to be uniformly dispersed. The average particles size is in close agreement with both the technique, i.e., as observed in TEM and the crystallite size calculated by the Scherrer equation (~ 31.0 nm) with the help of XRD technique. Further, the TEM diffraction ring (Figure 13b) confirms that the ferrite nanoparticles are in a well crystalline state [25].

The purpose of addition of HRP in the slurry of working electrode is because HRP enhance the intensity of weak electrochemical signal. Ferrocene act as stimulator. Grapheme was added into the slurry of working electrode to increase its conductivity and surface area of the electrode.

From the Tables 1 and 2, it is observed that OCP value of PBS buffer solution decreases on addition of 3.0×10^7 CFU of *V. vulnificus*. OCP value of PBS buffer solution increases on addition of Fe_3O_4 nanoparticles. OCP value of *V. vulnificus* decreases (0.238-0.226 V) on addition of Fe_3O_4 nanoparticles ($50 \mu\text{l ml}^{-1}$). It means that Fe_3O_4 nanoparticles are showing antibacterial properties and makes *V. vulnificus* as inactive. This may be due to the penetration of *V. vulnificus* deep inside the bacteria through bacterial cell wall and thus making it inactive.

Heating of samples to 70.0°C leads to decrease in the OCP value from 0.240 to 0.185 V with 3.0×10^7 CFU of *V. vulnificus* and from 0.228 to 0.180 V with 3.0×10^7 CFU of *V. vulnificus* and Fe_3O_4 nanoparticles ($50 \mu\text{l ml}^{-1}$). Heating of samples to 70.0°C makes bacterial cell inactive just like addition of nanoparticles which lowers its OCP value.

Thus, it is concluded that heating of samples to 70.0°C for 6.0 h (Table 2) and addition of Fe_3O_4 nanoparticles ($50 \mu\text{l ml}^{-1}$) at room temperature (Table 1) has the same effect, i.e. both results in decrease in OCP value of PBS buffer solution with 3.0×10^7 CFU of *V. vulnificus*. Hence, it is concluded that an OCP value of 0.240 V in phosphate buffer solution confirms the presence of *V. vulnificus* pathogenic bacteria. Heating of the samples up to 70.0°C for a definite period of time leads to decrease in OCP value. The addition of Fe_3O_4 nanoparticles also leads to decrease in OCP value, i.e. heating and additions of Fe_3O_4 nanoparticles have same effect on *V. vulnificus* which lowers its OCP value.

It is observed from Figure 2 that the current and potential behavior of pure PBS solution is different at 0.0 and 6.0 h of continuous stirring. The current value decreases with increase in potential value after 6 h of continuous stirring. It is also observed from Figure 3 that current value decreases with increase in the potential of PBS

buffer solution in the presence of Fe_3O_4 nanoparticles ($50 \mu\text{l ml}^{-1}$) after 6.0 h of continuous stirring. Similar types of results were observed in the case of samples containing *V. vulnificus* (Figure 4). The current and potential behavior of samples containing both Fe_3O_4 nanoparticles ($50.0 \mu\text{l ml}^{-1}$) and 3.0×10^7 CFU of *V. vulnificus* also shows decrease in current values after 6.0 h of continuous stirring (Figure 5).

It is observed from the Figure 6 that the value of current shows non-linear behavior with increase in potential value at initial time and after 6.0 h of continuous stirring. It is observed from the Figure 7 that the value of current first decrease and then increase and then becomes almost constant with increase in potential value in the presence of Fe_3O_4 nanoparticles at initial time. Current values show non-linear behavior after 6.0 h of heating at 70.0°C . Figure 8 shows that value of current initially decreases and then increase and thereafter remains almost constant with increase in potential value in the presence of 3.0×10^7 CFU of *Klebsiella pneumonia* in PBS solution at initial time. Current value decreases slightly after 6 h of heating.

5. CONCLUSION

Carbon (graphene) based working electrode having alkaline phosphatase, cellulose acetate, ferrocene, HRP, aqueous KOH and PVP was fabricated which when combined with Ag/AgCl reference and a platinum auxiliary electrode to form a three-electrode based electrochemical cell for the electrochemical detection of *V. vulnificus* as BWA. Fe_3O_4 nanoparticles were synthesized by sol-gel method. Characterization of Fe_3O_4 nanoparticles was carried out by using UV-visible, FTIR, XRD and TEM techniques. An UV-visible absorption band at the wavelength of 410.0 nm and a sharp absorption band at 600.0 cm^{-1} in FTIR spectra confirm the formation of ferrite nanoparticles. Heating of samples to 70.0°C for 6.0 h and addition of Fe_3O_4 nanoparticles ($50.0 \mu\text{l ml}^{-1}$) at room temperature has the same effect, i.e. both results in decrease in OCP value. The value of both current and potential decreases on addition of Fe_3O_4 nanoparticles ($50.0 \mu\text{l ml}^{-1}$). Continuous stirring of the samples of PBS and *V. vulnificus* in the presence of Fe_3O_4 nanoparticles for a definite time leads to decrease in current value. This may be due to escaping of Fe_3O_4 nanoparticles from bacterial cell thus making *V. vulnificus* again in active form. A constant OCP value of 0.240 V in phosphate buffer solution indicates the presence of *V. vulnificus* pathogenic bacteria in the sample.

6. ACKNOWLEDGMENT

We are very thankful to DRDO, New Delhi for providing us financial support for this research work.

7. REFERENCES

1. North Atlantic Treaty Organization, (1996) *NATO Handbook on the Medical Aspects of*

- NBC Defensive Operations, Part II, Biological*, Washington, DC: NATO AMedP-6(B).
- I. Karube, K. Hera, H. Matsuoka, S. Suzuki, (1982) Amperometric determination of total cholesterol in serum with use of immobilized cholesterol esterase and cholesterol oxidase, *Analytica Chimica Acta*, **139**: 127-132.
 - V. Veldhoven, P. P. Meyhi, G. P. Mannaerts, (1998) Enzymatic quantitation of cholesterol esters in lipid extract, *Analytical Biochemistry*, **258**: 152-155.
 - B. Shahnaz, S. Tada, T. Kajikawa, T. Ishida, K. Kawanishi, (1998) Automated fluorimetric determination of cellular cholesterol, *Annals of Clinical Biochemistry*, **345**: 665-670.
 - J. F. Kennedy, (1975) In: A. Wiseman, (Ed.), *Handbook of Enzyme Biotechnology*, New York: Chap John Wiley and Sons.
 - S. Singh, P. R. Solanki, B. D. Malhotra, (2006) Covalent immobilization of cholesterol esterase and cholesterol oxidase on polyaniline films for application to cholesterol biosensor, *Annals of Clinical Biochemistry*, **568**: 126-132.
 - J. F. Kennedy, (1985) *Handbook of Enzyme Technology*, New York: Marcel Dekker.
 - W. E. Lee, H. G. Thomson, J. G. Hall, R. E. Fulton, J. P. Wong, (1993) Characteristics of the biochemical detector sensor. Defence Research Establishment Suffield, Canada. Suffield Memorandum No.1402, p1-23.
 - C. Ercole, M. Del Gallo, M. Pantalone, S. Santucci, L. F. Mosiello, C. Laconi, A. Lepidi, (2002) A biosensor for *Escherichia coli* based on a potentiometric alternating biosensing (PAB) transducer, *Sensor Actuators B: Chemical*, **4163**: 1-5.
 - A. L. Ghindilis, P. Atanasov, P. Wilkins, E. Wilkins, (1998) A biosensor for *Escherichia coli* based on a potentiometric alternating biosensing (PAB) transducer, *Biosensors Bioelectronics*, **13**: 113-131.
 - E. L. Crowley, C. K. O'Sullivan, G. G. Guilbault, (1999) Increasing the sensitivity of listeria monocytogenes assays: Evaluating using ELISA and amperometric detection, *Analyst*, **124(3)**: 295-299.
 - B. Mirhabibollahi, J. L. Brooks, R. G. Kroll, (1990) A semi-homogeneous amperometric immunosensor for protein A-bearing *Staphylococcus aureus* in foods, *Applied Microbiology and Biotechnology*, **34**: 242.
 - J. L. Brooks, B. Mirhabibollahi, R. G. Kroll, (1990) Sensitive enzyme-amplified electrical immunoassay for protein A-bearing *S. aureus* in food, *Applied and Environmental Microbiology*, **56**: 3278-3284.
 - N. Nakamura, A. Shigematsu, T. Matsunaga, (1991) Electrochemical detection of viable bacteria in urine and antibiotic selection, *Biosensors and Bioelectronics*, **6**: 575.
 - J. L. Brook, B. Mirhabibollahi, R. G. Kroll, (1992) Experimental enzyme linked immunosensor for the detection of *Salmonella* in food, *Journal of Applied Microbiology*, **73**: 189-196.
 - H. J. Kim, H. P. Bennetto, M. A. Haqlablab, (1995) A novel liposome based electrochemical biosensor for the detection of haemolytic microorganisms, *Biotechnology Techniques*, **9(6)**: 389-394.
 - H. Kumar, R. Rani, (2013) Development of biosensor for the detection of biological warfare agents: Its issues challenges, *Science Progress*, **96(3)**: 294-308.
 - T. Koutzarova, S. Kolev, C. Ghelev, D. Paneva, I. Nedkov, (2006) Microstructural study and size control of iron oxide nanoparticles produced by microemulsion technique, *Physica Status Solidi (c)*, **3(5)**: 1302-1307.
 - X. J. Bard, L. R. Faulkner, (2000) *Electrochemical Methods: Fundamentals and Applications*, 2nd ed. New York: Wiley.
 - X. Chen, Y. Wang, J. Zhou, W. Yan, X. Li J. J. Hu, (2008) Electrochemical impedance immunosensor based on three-dimensionally ordered macroporous gold film, *Analytical Chemistry*, **80**: 2133-2140.
 - J. H. Meng, G. Q. Yang, L. M. Yan X. Y. Wang, (2005) Synthesis and characterization of magnetic nanometer pigment Fe₃O₄, *Dyes and Pigments*, **66**: 109-113.
 - A. Kaushik, R. Khan, P. R. Solanki, P. Pandey, J. Alam, S. Ahmad B. D. Malhotra, (2008) Iron oxide nanoparticles-chitosan composite based glucose biosensor, *Biosensors and Bioelectronics*, **24(4)**: 676-683.
 - R. Boistelle J. P. Astier. (1988) Crystallization mechanism in solutions, *Journal of Crystal Growth*, **90**: 14-30.
 - H. K. Moudgil, (2015) *A Textbook of Physical Chemistry*, 2nd ed. New Delhi: Prentice Hall of India, Pvt., Ltd., p648-650.
 - J. Wang, Q. Chen, C. Zheng, B. Hou. (2004) Magnetic-field-induced growth of single-crystalline Fe₃O₄ nanowires, *Advanced Materials*, **16(2)**: 137-140.

***Bibliographical Sketch**



Dr. Harish Kumar is Assistant Professor in the Department of Chemistry, Chaudhary Devi Lal University, Sirsa (Haryana) 125 055, India. He has published more than 58 papers and three books on Physical Chemistry. He is member of editorial board different scientific journals. His main sphere of interest is in electrochemistry and material science. He may be contacted at harimoudgil1@gmail.com.



Bhawana is a Project Fellow of DRDO in Department of Chemistry, Ch. Devi Lal University, Sirsa (Haryana) 125055, India, under the project entitled "Electrochemical Biosensors for the Detection of Biological Weapon." She completed her Master degree in Chemistry from Chaudhary Devi Lal University, Sirsa (Haryana) and Bachelor degree from Govt. National P.G. College, Sirsa (Haryana). She completed her Bachelor of Education from J. C. D. (PG) College of Education, Sirsa (Haryana). She has attended many Conferences, Seminars, and Workshops. She has won many prizes in University Youth Festivals and other cultural and literary events. She may be contacted at sejalsingla172@gmail.com.